Local Geometry Trends and Torsional Sensitivity in *N*-Formyl-L-alanyl-L-alanine Amide and the Limitations of the Dipeptide Approximation

Ching-Hsing Yu and Lothar Schäfer[†]

Department of Chemistry and Biochemistry, University of Arkansas, Fayetteville, Arkansas 72701

Michael Ramek*[,‡]

Institut für Physikalische und Theoretische Chemie, Technische Universität Graz, A-8010 Graz, Austria

Received: June 25, 1999

Based on a database of 11 664 RHF/4-21G ab initio gradient-optimized structures of *N*-formyl-L-alanyl-L-alanine amide (ALA-ALA), the local geometries and torsional sensitivity of this compound were analyzed to test the dipeptide approximation frequently used in peptide conformational analyses. This database was generated by optimizing the geometries of this compound at grid points in its four-dimensional (ϕ_1,ψ_1,ϕ_2,ψ_2) conformational space defined by 40° increments along the outer torsions ϕ_1 and ψ_2, and by 30° increments along the inner torsions ψ_1 and ϕ_2. Using cubic spline functions, the grid structures were then used to construct analytical representations of complete surfaces of the structural parameters of ALA-ALA, and of their gradients, in (ϕ_1,ψ_1,ϕ_2,ψ_2) space. Analysis of the structural surfaces shows not only that the structure of a given residue in a peptide chain depends acutely on the conformational state of a neighboring residue but also that the interresidue effects differ, depending on whether they are transmitted from right to left or from left to right in the peptide chain. Structural gradients are a qualitative measure of the torsional sensitivity, and therefore of the density of states and contributions to vibrational entropy. Analyses of the gradient surfaces show that the density of states in a residue is significantly affected by the dynamics of a neighboring residue. This opens the possibility of dynamic entropic conformational steering in extended peptide chains, i.e., the generation of free energy contributions from dynamic effects of one part of a molecule on another, possibly stabilizing a conformational region of a PES whose static energy profile is less favorable compared to other regions. The gradient trends illustrate how the overall stability of a complex molecule is not only a function of how the static energy minima of its isolated subunits combine but also of how the dynamics of the subunits interact with one other. These interactions between individual residues represent a hidden cooperative effect that is not apparent at all in the dynamics of isolated dipeptide units.

Introduction

In the recent past there has been considerable interest in the quantum chemical treatment of model tripeptides,[1−10] specifically in *N*-acetyl-L-alanyl-L-alanine-*N*′-methyl amide[11−14] and *N*-formyl-L-alanyl-L-alanine amide (ALA-ALA, henceforth; Figure 1).[13,15−21] The results for such compounds are often considered as paradigms for larger systems, such as oligopeptides and proteins[22−42] which are not yet readily accessible to advanced computational methods.

In this context, the "dipeptide approximation" has frequently been applied,[43−51] which postulates that the conformational properties of the *i*-th residue of a peptide chain, particularly the values of the torsional angles ϕ_i and ψ_i (Figure 1), depend mainly on the nature of the residue R_i and are largely independent of the neighboring pairs, ϕ_{i-1},ψ_{i-1} and ϕ_{i+1},ψ_{i+1}. More specifically,[51] "the interactions associated with rotations of a ϕ_i,ψ_i pair are largely independent of the angles assumed by the neighboring pairs ϕ_{i-1},ψ_{i-1} and ϕ_{i+1},ψ_{i+1}." Since short-range interactions are highly important in the folding of polypeptide chains, the dipeptide model has been rather effective, in spite of the fact that it neglects cooperative phenomena and long-range interactions in polymer chains.

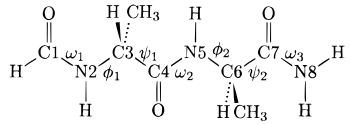

Figure 1. *N*-Formylalanylalanine amide. Notation for backbone torsional angles.

The purpose of this paper is an assessment of the limitations of the dipeptide approximation, analyzing conformational geometry trends obtained by ab initio calculations for ALA-ALA and extending a related analysis of conformational energies.[21] In the latter it was found[21] that the conformational energy surface of a residue in a peptide chain can be significantly affected by conformational changes in a neighboring residue. In addition, it was found that the positions of energy minima of tripeptides cannot be reliably derived from the structural features of dipeptides. Within the framework of the dipeptide approximation, Perczel et al.[18,20] recently attempted to predict the energy minima of ALA-ALA from 81 trial conformations which were generated on the basis of nine "standard orientations" that the authors determined for model dipeptides. These 81 conformations converged to 49 different energy minima in RHF/3-21G conformational space,[20] which is two minima less than found by the direct RHF/4-21G grid search[21] of the PES of ALA-ALA. The discrepancy is not due[21] to differences

[†] E-mail: schafer@protein.uark.edu.
[‡] E-mail: ramek@ptc.tu-graz.ac.at.

10.1021/jp992166w CCC: $18.00
Published on Web 09/29/1999

TABLE 1: Backbone Bond Lengths (Å)[a] and Relative Energies *E* (kcal/mol) of the RHF/6-31G* Optimized Conformational Energy Minima[b] of *N*-Formyl-L-alanyl-L-alanine Amide

conformer	C1−N2	N2−C3	C3−C4	C4−N5	N5−C6	C6−C7	C7−N8	*E*
$\gamma'\gamma'$	1.344	1.457	1.535	1.342	1.459	1.536	1.350	0.000
$\beta_S\beta_S$	1.342	1.444	1.526	1.342	1.444	1.526	1.347	0.082
$\beta_S\gamma'$	1.344	1.443	1.524	1.343	1.459	1.535	1.349	0.329
$\delta_R\delta_R$	1.351	1.457	1.530	1.347	1.450	1.533	1.346	1.599
$\gamma'\delta_R$	1.344	1.458	1.536	1.357	1.454	1.530	1.349	1.829
$\zeta\gamma'$	1.360	1.452	1.530	1.342	1.458	1.535	1.349	2.071
$\gamma'\beta_S$	1.348	1.455	1.532	1.343	1.443	1.525	1.351	2.100
$\delta_R\beta_S$	1.355	1.451	1.531	1.341	1.442	1.525	1.349	2.215
$\gamma\gamma'$	1.344	1.462	1.534	1.339	1.458	1.536	1.350	2.273
$\gamma'\delta_L$	1.344	1.457	1.538	1.341	1.461	1.533	1.348	2.468
$\beta_S\zeta$	1.344	1.442	1.527	1.355	1.455	1.531	1.353	2.588
$\beta_P\delta_L$	1.345	1.448	1.533	1.348	1.457	1.535	1.349	2.835
$\beta_S\gamma$	1.344	1.443	1.526	1.342	1.464	1.533	1.345	3.086
$\gamma'\epsilon$	1.348	1.457	1.532	1.355	1.449	1.539	1.355	3.243
$\epsilon\delta_R$	1.344	1.455	1.541	1.347	1.451	1.533	1.346	3.276
$\gamma\beta_P$	1.347	1.454	1.540	1.348	1.451	1.534	1.347	3.481
$\delta_L\gamma'$	1.357	1.459	1.533	1.342	1.458	1.534	1.349	3.651
$\alpha_L\beta_S$	1.354	1.458	1.534	1.343	1.441	1.525	1.348	3.996
$\gamma'\alpha_L$	1.344	1.460	1.537	1.351	1.457	1.532	1.358	4.105
$p\beta_P$	1.352	1.462	1.524	1.367	1.442	1.534	1.349	4.226
$\beta_S\alpha_L$	1.344	1.442	1.525	1.354	1.461	1.533	1.356	4.395
$\gamma' p$	1.341	1.460	1.538	1.345	1.455	1.525	1.356	4.372
$\delta_R\gamma$	1.359	1.453	1.533	1.339	1.463	1.533	1.345	4.507
$\epsilon\gamma'$	1.354	1.451	1.539	1.345	1.459	1.535	1.351	4.593
$\delta_L\delta_R$	1.344	1.464	1.534	1.351	1.452	1.531	1.349	4.693
$\gamma\delta_L$	1.343	1.462	1.535	1.338	1.461	1.533	1.347	4.808
$\zeta\epsilon$	1.349	1.456	1.529	1.366	1.449	1.540	1.349	4.834
$\delta_L\beta_S$	1.346	1.459	1.532	1.341	1.443	1.525	1.351	4.927
$\beta_S\epsilon$	1.343	1.443	1.524	1.353	1.453	1.538	1.355	4.938
$\alpha_L\delta_L$	1.352	1.462	1.535	1.349	1.456	1.535	1.350	5.037
$\epsilon\beta_S$	1.355	1.452	1.539	1.343	1.444	1.525	1.350	5.070
$p\beta_S$	1.354	1.460	1.525	1.350	1.443	1.525	1.347	5.134
$p\gamma'$	1.360	1.461	1.525	1.349	1.460	1.535	1.348	5.364
$\beta_S p$	1.343	1.443	1.526	1.351	1.461	1.524	1.366	5.471
$\alpha_L\delta_R$	1.357	1.460	1.535	1.359	1.455	1.530	1.353	6.136
$\gamma\alpha_L$	1.343	1.463	1.535	1.351	1.458	1.532	1.357	6.111
$\delta_R\alpha_L$	1.357	1.453	1.533	1.354	1.460	1.532	1.359	6.703
$\alpha_L\gamma$	1.359	1.459	1.536	1.344	1.463	1.534	1.346	6.792
$\gamma\epsilon$	1.343	1.462	1.531	1.345	1.451	1.539	1.359	7.140
$\epsilon\delta_L$	1.352	1.454	1.540	1.339	1.465	1.532	1.345	7.445
$\delta_R p$	1.358	1.453	1.532	1.355	1.460	1.524	1.366	7.848
$p\gamma$	1.359	1.461	1.526	1.350	1.464	1.534	1.345	8.201
$\delta_L p$	1.352	1.463	1.537	1.344	1.456	1.527	1.359	8.257
$p\epsilon$	1.354	1.460	1.522	1.367	1.456	1.537	1.354	9.441
$\epsilon\epsilon$	1.357	1.450	1.536	1.351	1.452	1.538	1.356	9.542
$p\alpha_L$	1.361	1.462	1.527	1.357	1.459	1.533	1.356	10.332
pp	1.359	1.462	1.526	1.354	1.457	1.525	1.369	11.052

[a] See Figure 1 for atom numbers. [b] See ref 21 for notation.

between the rather similar 3-21G[52] and 4-21G[53] basis sets, but is indicative of the fundamental inability of the dipeptide model to predict all essential features of the potential energy surface (PES) of larger peptides. In this case, specifically, the two missing conformers fall into the same standard dipeptide conformational range as two other conformers,[18,20] but they are separated from these by reaction paths with distinct saddle points.[21]

In the current paper the validity of the dipeptide approximation will be further explored by focusing on the local geometries[54] and the torsional sensitivity[55,56] of residues in a peptide chain. Both will be seen to depend acutely on the conformational state of neighboring residues.

Computational Procedures

For the present study we have generated a structural database consisting of 11 664 ab initio gradient-optimized structures of ALA-ALA. This database was obtained by optimizing the geometries of this compound at grid points in its four-dimensional (ϕ_1,ψ_1,ϕ_2,ψ_2) conformational space (Figure 1) defined by 40° increments along the outer torsions ϕ_1 and ψ_2, and by 30° increments along the inner torsions ψ_1 and ϕ_2.[21] The smaller step size for the latter was chosen because the properties of the central peptide bond are of particular interest. At each of the $9 \times 12 \times 12 \times 9 = 11\,664$ grid points, geometry optimizations were performed via RHF/4-21G[53] calculations, in which the torsions ϕ_1, ψ_1, ϕ_2, and ψ_2 were kept constant while all other structural parameters were relaxed without any constraints. The orientation of the torsions ω_1 (i.e., H−C−N−C) and ω_2 was trans in all cases.

In order to evaluate the results of the ab initio calculations, an auxiliary program was written using natural cubic spline functions to generate an analytical approximation of the PES of ALA-ALA from the 11 664 grid points. With the help of this program it was possible to locate the local minima, which were subsequently optimized in RHF/4-21G[53] and RHF/6-31G*[57,58] calculations. The spline function generated analytical representation of the PES can be used for calculating complete surfaces of the torsional dependence of bond lengths and angles on ϕ and ψ. Specifically, the conformational properties of the two amino acid residues of ALA-ALA can be explored when one of them is kept in a constant orientation while the other is

TABLE 2: Backbone Valence Angles (deg)[a] and Relative Energies *E* (kcal/mol) of the RHF/6-31G* Optimized Conformational Energy Minima[b] of *N*-Formyl-L-alanyl-L-alanine Amide

conformer	C1−N2−C3	N2−C3−C4	C3−C4−N5	C4−N5−C6	N5−C6−C7	C6−C7−N8	*E*
$\gamma'\gamma'$	123.09	110.11	114.90	123.14	109.88	114.38	0.000
$\beta_S\beta_S$	122.56	107.38	115.47	122.44	107.25	115.48	0.082
$\beta_S\gamma'$	122.23	107.53	115.83	123.34	109.53	114.45	0.329
$\delta_R\delta_R$	121.51	114.45	117.40	123.37	113.75	117.53	1.599
$\gamma'\delta_R$	123.14	109.59	114.29	121.74	112.64	116.70	1.829
$\zeta\gamma'$	122.36	113.24	117.26	123.02	109.94	114.44	2.071
$\gamma'\beta_S$	122.45	108.91	115.21	121.88	107.79	115.32	2.100
$\delta_R\beta_S$	123.05	114.20	117.30	121.95	107.28	115.45	2.215
$\gamma\gamma'$	127.10	113.91	117.44	122.92	109.95	114.38	2.273
$\gamma'\delta_L$	123.07	110.13	114.44	127.15	115.25	117.38	2.468
$\beta_S\zeta$	122.16	107.53	115.15	122.65	112.29	116.54	2.588
$\beta_P\delta_L$	120.19	109.92	115.49	124.00	114.05	116.94	2.835
$\beta_S\gamma$	122.20	107.69	115.28	127.41	114.52	117.17	3.086
$\gamma'\epsilon$	122.38	108.21	114.68	119.89	109.51	117.08	3.243
$\epsilon\delta_R$	121.56	108.87	117.65	123.07	114.35	117.78	3.276
$\gamma\beta_P$	120.56	108.69	117.40	122.88	114.16	117.80	3.481
$\delta_L\gamma'$	122.83	113.03	116.79	122.82	109.46	114.27	3.651
$\alpha_L\beta_S$	123.23	112.76	116.07	122.08	107.23	115.45	3.996
$\gamma'\alpha_L$	123.27	110.85	114.83	123.11	113.39	116.10	4.105
$p\beta_P$	121.28	107.21	115.44	118.53	109.43	115.82	4.226
$\beta_S\alpha_L$	122.23	107.54	115.64	122.93	113.17	116.26	4.395
$\gamma' p$	123.84	109.57	113.75	123.55	110.59	116.92	4.372
$\delta_R\gamma$	122.65	113.82	116.88	127.08	114.25	117.13	4.507
$\epsilon\gamma'$	120.73	109.60	117.50	122.64	109.49	114.55	4.593
$\delta_L\delta_R$	127.16	114.63	117.11	122.45	113.85	117.11	4.693
$\gamma\delta_L$	127.15	114.21	117.02	126.88	115.15	117.41	4.808
$\zeta\epsilon$	122.23	107.78	114.89	119.37	109.10	117.09	4.834
$\delta_L\beta_S$	127.01	115.48	118.23	121.28	108.21	115.15	4.927
$\beta_S\epsilon$	122.27	107.54	115.59	120.70	109.44	117.49	4.938
$\alpha_L\delta_L$	122.86	112.78	116.29	123.59	113.78	116.77	5.037
$\epsilon\beta_S$	121.00	109.49	117.38	121.35	107.37	115.40	5.070
$p\beta_S$	121.77	110.55	116.20	122.19	107.14	115.58	5.134
$p\gamma'$	121.62	109.94	116.36	122.89	109.13	114.42	5.364
$\beta_S p$	122.31	107.50	115.35	121.71	109.81	115.92	5.471
$\alpha_L\delta_R$	122.44	112.76	115.89	121.57	112.57	116.61	6.136
$\gamma\alpha_L$	127.03	113.06	116.99	122.32	113.21	115.96	6.111
$\delta_R\alpha_L$	122.90	113.73	117.10	122.32	113.47	116.39	6.703
$\alpha_L\gamma$	122.04	112.22	115.59	126.79	113.26	116.79	6.792
$\gamma\epsilon$	127.34	114.52	117.65	120.60	109.48	117.48	7.140
$\epsilon\delta_L$	121.45	109.08	118.00	126.41	114.37	117.29	7.445
$\delta_R p$	122.50	113.01	116.70	120.72	110.10	116.05	7.848
$p\gamma$	121.57	110.46	116.02	126.99	114.61	117.15	8.201
$\delta_L p$	124.93	114.88	116.62	126.38	108.96	116.11	8.257
$p\epsilon$	121.64	110.38	116.35	119.36	109.35	117.67	9.441
$\epsilon\epsilon$	121.27	109.87	117.25	120.52	109.24	117.46	9.542
$p\alpha_L$	121.79	109.77	116.07	123.44	113.80	116.51	10.332
pp	121.83	109.99	115.99	121.85	108.83	115.63	11.052

[a] See Figure 1 for atom numbers. [b] See ref 21 for notation.

allowed to move freely. Throughout this paper we will refer to the former as the *constrained residue*, and to the latter, as the *moving residue*. As an additional feature, it is a particular strength of the complete parameter surfaces that they make it possible to calculate parameter gradients at each point in ϕ,ψ-space. The parameter gradients provide an effective measure of the torsional sensitivity[55,56] of the system.

Results and Discussion

(a) Notation. For the purposes of this paper the following notation was adopted. The terms *residue 1* and *residue 2* are used to denote the fragments $-NH-C_\alpha H(CH_3)-C'O-$ with N2, C3, C4 and N5, C6, C7, respectively (Figure 1). The shorthand "*Yi.xx.j*" (where $i, j = 1, 2$) is used for the property *Y* of residue *i* (for example, *Y* can be a bond length or bond angle of interest), when residue *j* is the moving residue, i.e., it is allowed to move in ϕ_j,ψ_j-space, while the other residue (i.e., residue $i = 3 - j$) is the constrained residue; i.e., its ϕ,ψ torsional angles are kept constant at a point defined by the two-letter symbol *xx*. The latinicized symbols "al", "ar", "bt", and "br" are used for *xx*, which denote the regions α_L, α_R, β_S, and the bridge region δ_R, respectively. In agreement with a convention generally accepted in protein crystallography,[62] we have selected $\phi = \psi = 55°$ for al, $\phi = -75°$ and $\psi = -45°$ for ar, $\phi = -165°$ and $\psi = 165°$ for bt, and $\phi = -90°$ and $\psi = 0°$ for br.

The results of our analyses are presented in Tables 1−7 and in Figures 2−12. Selected structural parameters of the RHF/6-31G* optimized conformational energy minima of ALA-ALA are presented in Tables 1 and 2. Differences between maximum and minimum values encountered on various surfaces are presented in Tables 3−5. Root mean square (rms) deviations between bond lengths and angles of various ϕ,ψ-surfaces are given in Tables 6 and 7.

Using the atom numbering given in Figure 1, Figures 2 and 3 show the parameter surfaces $N-C_\alpha-C'$1.al.2 (i.e., the dependence of the $N-C_\alpha-C'$ angle in residue 1 on ϕ_2 and ψ_2) and $N-C_\alpha-C'$2.al.1 (i.e., the functional dependence of the $N-C_\alpha-C'$ angle in residue 2 on ϕ_1 and ψ_1), respectively. In Figure 4 differences between 2.bt.1 and 2.ar.1, 2.br.1, and 2.al.1, respectively, are given for the bond distances $C_\alpha-C'$ and $N-C_\alpha$ and the valence angle $N-C_\alpha-C'$.

TABLE 3: Maximum and Minimum Values (in deg) of the Intraresidue Valence Angles N−C_α−C′, C_α−C=O, and N−C_α−C_β (deg) within the Moving Residue

parameter	maximum	minimum	difference
N−C_α−C′1.al.1	123.4	103.1	20.2
N−C_α−C′1.ar.1	123.0	103.1	19.9
N−C_α−C′1.br.1	123.3	102.0	21.3
N−C_α−C′1.bt.1	123.9	103.0	20.9
C_α−C=O1.al.1	125.5	114.4	11.1
C_α−C=O1.ar.1	125.7	114.6	11.1
C_α−C=O1.br.1	125.7	114.4	11.3
C_α−C=O1.bt.1	125.5	113.4	12.1
N−C_α−C_β1.al.1	115.7	107.1	8.6
N−C_α−C_β1.ar.1	115.6	107.0	8.6
N−C_α−C_β1.br.1	115.7	106.9	8.8
N−C_α−C_β1.bt.1	115.4	106.9	8.4
C_α−C=O2.al.2	127.8	114.3	13.5
C_α−C=O2.ar.2	127.8	114.5	13.3
C_α−C=O2.br.2	127.0	114.3	12.7
C_α−C=O2.bt.2	126.7	114.3	12.4
N−C_α−C_β2.al.2	116.2	106.1	10.1
N−C_α−C_β2.ar.2	116.3	106.0	10.3
N−C_α−C_β2.br.2	116.5	106.7	9.8
N−C_α−C_β2.bt.2	116.3	106.8	9.5
N−C_α−C′2.al.2	123.8	103.1	20.6
N−C_α−C′2.ar.2	123.5	102.7	20.8
N−C_α−C′2.br.2	124.0	102.7	21.4
N−C_α−C′2.bt.2	123.9	102.7	21.2

TABLE 4: Maximum and Minimum Values (in deg) of the Intraresidue Valence Angles N−C_α−C′, C_α−C=O, and N−C_α−C_β (deg) within the Constrained Residue

parameter	maximum	minimum	difference
N−C_α−C′2.al.1	112.3	109.2	3.1
N−C_α−C′2.ar.1	113.5	110.6	2.9
N−C_α−C′2.br.1	115.3	112.3	3.0
N−C_α−C′2.bt.1	108.2	105.9	2.4
C_α−C=O2.al.1	123.3	121.0	2.3
C_α−C=O2.ar.1	122.1	120.1	2.0
C_α−C=O2.br.1	119.7	118.2	1.5
C_α−C=O2.bt.1	123.0	121.3	1.6
N−C_α−C_β2.al.1	112.9	111.4	1.5
N−C_α−C_β2.ar.1	110.3	109.4	0.9
N−C_α−C_β2.br.1	111.8	110.0	1.8
N−C_α−C_β2.bt.1	112.1	110.9	1.2
N−C_α−C′1.al.2	112.2	108.7	3.5
N−C_α−C′1.ar.2	113.7	110.3	3.4
N−C_α−C′1.br.2	115.0	113.0	2.0
N−C_α−C′1.bt.2	106.8	106.2	0.7
C_α−C=O1.al.2	123.6	119.8	3.8
C_α−C=O1.ar.2	122.2	117.8	4.3
C_α−C=O1.br.2	120.0	116.1	3.9
C_α−C=O1.bt.2	122.2	119.2	3.0
N−C_α−C_β1.al.2	113.0	112.1	0.8
N−C_α−C_β1.ar.2	110.8	109.8	1.0
N−C_α−C_β1.br.2	111.3	110.3	1.0
N−C_α−C_β1.bt.2	111.9	111.4	0.6

Some sample surfaces of the magnitudes of structural gradients are presented in Figures 5−12. In the latter surfaces of the type $[(\partial Y/\partial\phi_i)^2 + (\partial Y/\partial\psi_i)^2]^{1/2}$ are given as functions of ϕ_1 and ψ_1 or, alternatively, of ϕ_2 and ψ_2, with Y = N−C_α−C′1.bt.2, N−C_α−C′1.al.2, N−C_α−C′1.ar.2, N−C_α−C′1.br.2, N−C_α−C′2.bt.1, N−C_α−C′2.al.1, N−C_α−C′2.ar.1, and N−C_α−C′2.br.1, respectively.

(b) Trends in Local Geometries. Within the framework of keeping one residue at constant values of ϕ and ψ while allowing the other to move, two categories of data can be produced from our database. In the first the geometry parameters of the moving residue are monitored as functions of its own ϕ and ψ torsional angles. That is, the resulting properties are of the type *Yi.xx.i*. The properties of the second category are of

TABLE 5: Maximum and Minimum Values of the Intraresidue Bond Lengths C_α−C′ and N−C_α (Å) within the Constrained Residue

parameter	maximum	minimum	difference
C_α−C′2.al.1	1.543	1.537	0.006
C_α−C′2.ar.1	1.535	1.528	0.006
C_α−C′2.br.1	1.538	1.531	0.006
C_α−C′2.bt.1	1.527	1.523	0.005
N−C_α2.al.1	1.478	1.467	0.011
N−C_α2.ar.1	1.474	1.459	0.015
N−C_α2.br.1	1.469	1.456	0.013
N−C_α2.bt.1	1.461	1.451	0.009
C_α−C′1.al.2	1.554	1.530	0.024
C_α−C′1.ar.2	1.545	1.525	0.020
C_α−C′1.br.2	1.550	1.531	0.019
C_α−C′1.bt.2	1.539	1.522	0.017
N−C_α1.al.2	1.478	1.465	0.013
N−C_α1.ar.2	1.474	1.460	0.014
N−C_α1.br.2	1.468	1.458	0.010
N−C_α1.bt.2	1.456	1.454	0.002

TABLE 6: Root Mean Square Deviations between Bond Lengths (Å) and Angles (deg) on the ϕ,ψ-Surfaces of ALA and ALA-ALA[a]

surface	C_α−C′	N−C_α	N−C_α−C′
1.al.1	0.0011	0.0023	0.64
1.ar.1	0.0018	0.0022	0.67
1.br.1	0.0015	0.0024	0.68
1.bt.1	0.0020	0.0022	0.63
2.al.2	0.0018	0.0028	0.83
2.ar.2	0.0015	0.0028	0.75
2.br.2	0.0014	0.0026	0.75
2.bt.2	0.0011	0.0022	0.53

[a] RMS deviations between sets of structural parameter of the model dipeptide *N*-acetyl-*N*′-methylalanine amide (ALA) and ALA-ALA. The sets of parameters consist of the HF/4-21G ab initio optimized bond lengths C_α−C′ and N−C_α, and the angles N−C_α−C′ calculated at 5° grid points in the ϕ,ψ-spaces of ALA and ALA-ALA. For the latter, the notation *i.xx.j* denotes sets of parameters of residue *i* (i = 1 or 2) that are found in ALA-ALA as one moves from one grid point to the next on the ϕ,ψ-surface of residue *j* (j = 1 or 2), while the torsions ϕ and ψ of the residue *i* other than *j* are being held fixed at conformation *xx* (where *xx* = al, ar, br, or bt, corresponding to α_L(ϕ=55, ψ=55), α_R(ϕ=−75, ψ=−45), δ_R(ϕ=−90, ψ=0), or β(ϕ=−165, ψ=165), respectively).

type *Yi.xx.j*, where $j \neq i$; that is, the changes in the parameters of the constrained residue *i* are monitored as functions of ϕ_j and ψ_j. While the first category (*i.xx.i*, i = 1 or 2) is comparable to parameter changes encountered in isolated model dipeptides, the latter (*i.xx.j*, $i \neq j$ = 1, 2) is a direct test of the accuracy of the dipeptide approximation.

The concept of "local geometry" was originally introduced[54] in order to emphasize the importance of local perturbations in affecting minimum energy geometries. Molecular geometries typically are local in the sense that they depend on where a given molecule is on its PES. The concept is in contrast to invariant and so-called "standard geometries". By employing the latter one attempts to propose a set of average structural parameters which are invariant at different locations of the PES, and characteristic and frequently recurring atom groups are given idealized, but inaccurate geometries. For example, a number of proposals for standard geometries of peptide systems have been published in the literature.[59−62] They all neglect the fact that the bond lengths and angles in such systems can vary significantly with torsional angles.

In the current case the magnitudes of the changes in structural parameters can be seen from the data presented in Tables 1 and 2 for the energy minima of ALA-ALA, and from the differences between maximum and minimum parameter values on various

TABLE 7: Root Mean Square Deviations between Bond Lengths (Å) and Angles (deg) Calculated for the Same Values of ϕ, ψ on Different Conformational Surfaces of ALA-ALA[a]

diff	$C_\alpha-C'$	$N-C_\alpha$	$N-C_\alpha-C'$
1.al.1−1.ar.1	0.0016	0.0017	0.41
1.al.1−1.br.1	0.0014	0.0024	0.52
1.al.1−1.bt.1	0.0019	0.0033	0.45
1.ar.1−1.br.1	0.0012	0.0016	0.42
1.ar.1−1.bt.1	0.0009	0.0034	0.45
1.br.1−1.bt.1	0.0015	0.0031	0.52
2.al.2−2.ar.2	0.0016	0.0047	0.94
2.al.2−2.br.2	0.0017	0.0045	0.97
2.al.2−2.bt.2	0.0013	0.0039	0.75
2.ar.2−2.br.2	0.0007	0.0012	0.64
2.ar.2−2.bt.2	0.0011	0.0041	0.72
2.br.2−2.bt.2	0.0010	0.0038	0.64
1.al.1−2.al.2	0.0017	0.0040	0.85
1.ar.1−2.ar.2	0.0015	0.0041	0.74
1.br.1−2.br.2	0.0016	0.0039	0.81
1.bt.1−2.bt.2	0.0017	0.0033	0.70
1.al.2−2.al.1	0.0040	0.0032	0.88
1.ar.2−2.ar.1	0.0041	0.0038	0.68
1.br.2−2.br.1	0.0048	0.0033	0.52
1.bt.2−2.bt.1	0.0040	0.0016	0.39

[a] The bond lengths $C_\alpha-C'$ and $N-C_\alpha$ and the angle $N-C_\alpha-C'$ were calculated at 5° grid points in the ϕ,ψ-spaces of ALA-ALA. The notation *i.xx.j* is the same as that of Table 6. The dual notation *i.xx.j*−*k.xx.l* identifies the two parameter sets for which the rms deviations were calculated.

parameter surfaces given in Table 3. From the latter it appears that parameter changes within a moving residue are largest for $N-C_\alpha-C'$ angles, but nonnegligible for other backbone angles of ALA-ALA.

For a realistic evaluation of the structural data used in this study, it should be pointed out that peptide structural trends obtained by RHF/4-21G geometry optimizations are rather accurate. For example, HF/4-21G and MP2/6-311G** geometry trends in amino acids and peptides have been compared and found to be very similar.[64] Furthermore, HF/4-21G geometries of parameters of the kind considered here are generally characterized by differences to experimental structures[65,66] which are constant, and therefore predictable. In the case of peptide $N-C_\alpha-C'$ angles, specifically, RHF/4-21G values were found in close agreement (rms deviations of 1.3°) with average values obtained from protein crystal structures.[67,68] Thus, the computational procedures applied to ALA-ALA in this study are sufficient for the purpose of this paper.

The breakdown of the dipeptide approximation is apparent from the data presented in Tables 4 and 5, presenting changes in bond lengths and angles within the constrained residue. That is, these changes occur in a given residue due to conformational motion in a neighboring residue in the peptide chain. Overall, these changes are smaller than those encountered within the moving residue (up to 3.5° for $N-C_\alpha-C'$, 4.3° for $C_\alpha-C'=O$, and 1.8° for $N-C_\alpha-C_\beta$), but it is obvious that they are not negligible.

The same result is suggested by Figures 2−4. From Figures 2 and 3 it is apparent not only that the $N-C_\alpha-C'$ angle in a residue depends on the conformational state of the neighboring residue but also that the interresidue effects from a neighbor in the chain to the right differ from those transmitted from a neighbor to the left. The same is apparent from Figure 4 (differences of type *Y*2.*xx*.1−*Y*2.*yy*.1, for $Y = N-C_\alpha$, $C_\alpha-C'$, and $N-C_\alpha-C'$ at different locations, $xx \neq yy$). Again, interresidue effects transmitted from right to left differ from those transmitted from left to right.

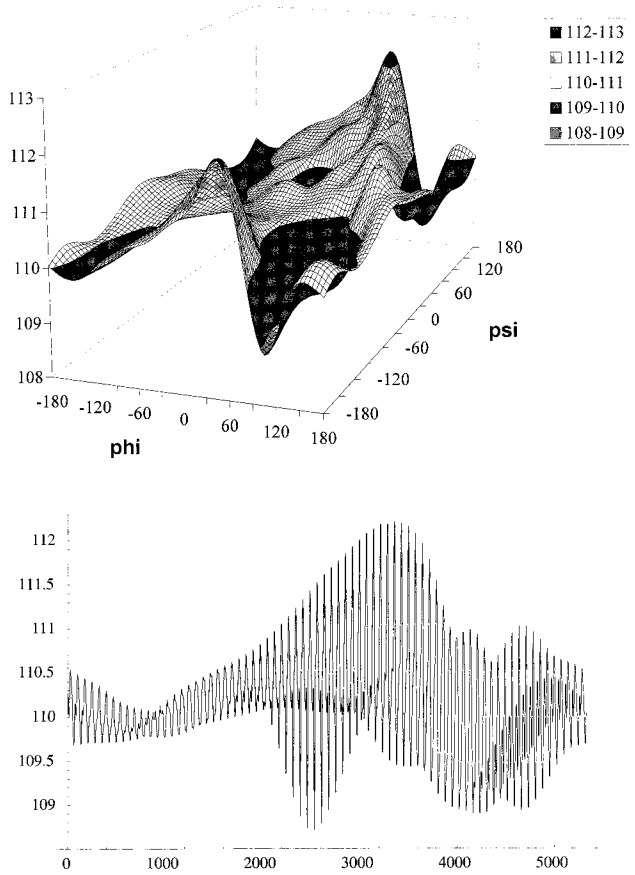

Figure 2. $N-C_\alpha-C'$1.al.2 surface (see the text for the *Yi.xx.j* notation). The variation of $N-C_\alpha-C'$ in residue 1 at 5° grid points is shown in ϕ_2,ψ_2-space. The upper graph shows a projection of the three-dimensional rendering, and the lower graph shows a linearized version of the same surface. In the latter, values of $N-C_\alpha-C'$ are shown as a function of the numbering of the 5° grid points in ϕ_2,ψ_2-space. Grid point numbering was started with the point at $\phi_2 = \psi_2 = -180°$ and increased from −180° to 180°, moving along the ψ-axis first.

Interresidue structural effects are also apparent from Tables 6 and 7. Table 6 lists rms deviations between parameters on the surfaces of a moving residue in ALA-ALA and on the corresponding RHF/4-21G surfaces of the isolated ALA residue in the model dipeptide *N*-acetyl-*N*′-methylalanine amide.[55] The magnitudes of the deviations are on the order of a few thousandths of an Å for bond lengths and 0.5°− 0.8° for $N-C_\alpha-C'$. Deviations of similar magnitude are found in Table 7 for differences between bond lengths and angles of ALA-ALA calculated for the same values of ϕ and ψ on different conformational surfaces.

(c) Torsional Sensitivity. Torsional sensitivity (TS)[55,56] is a measure of the extent to which the internal coordinates and nonbonded distances of a given molecule will change when the backbone torsional angles change. TS in a conformational region is high when small amplitude torsional motions around a given point in torsional space lead to large changes in bonded and nonbonded distances; TS is low when internal coordinates and nonbonds are not significantly affected by even large-amplitude torsional motions. A previous analysis has shown[55,56] that, in *n*-pentane-like structures, TS is not uniform but, rather, there are two conformational regions of maximum TS in ϕ,ψ-space situated at (ϕ,ψ) equal to (+40°, +40°) {or (−40°, −40°) by symmetry} and at (+90°, −90°) {or (−90°, +90°)}. The former is close to the GG region of saturated organic compounds (+60°, +60°) and to the helical regions of peptides and proteins ($\phi =$

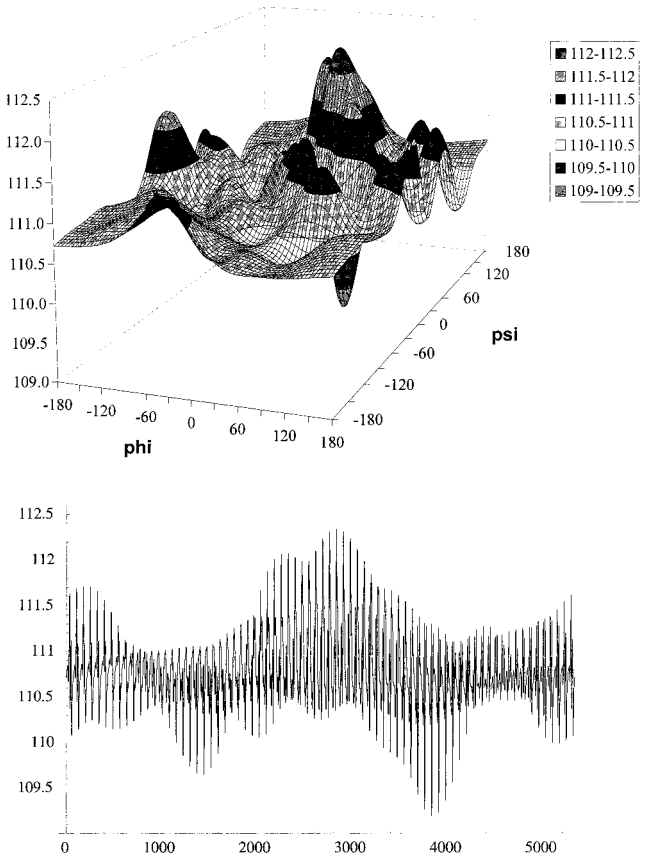

Figure 3. N−C_α−C′2.al.1 surface as a function of ϕ_1 and ψ_1. For details see Figure 2.

−60°, $\psi = -40°$), while the latter is encountered in the $C7^{eq}$ region of peptides. At the same time, minimum TS is found[55,56] in the vicinity of (180°, 180°), i.e., in all extended structures, such as the TT region of hydrocarbons and the β-regions of proteins.

TS is a constitutional property of nonlinear A-B-C-D-E-... bond chains that provides a basis for a physically significant classification of characteristic regions of the PES of a given molecule, because TS can be related to conformational entropy. In regions of low TS, potential energy wells are typically flat, there is a high density of states, and contributions to vibrational entropies are large. Vice versa, in regions of high TS, potential wells are characteristically steep, there is a low density of states, and contributions to vibrational entropies are small. Thus, the extended forms of complex molecules have a constitutional free energy advantage over puckered forms.

Information on TS is contained in structural gradients. In peptides, gradient magnitude for a backbone structural parameter Y is given by $[(\partial Y/\partial\phi)^2 + (\partial Y/\partial\psi)^2]^{1/2}$. When the magnitude of a gradient at a given point in ϕ,ψ-space is large, TS at this point is high; i.e., relatively small changes in torsional angles will lead to large changes in structural parameters or nonbonded distances. Vice versa, in regions of low TS, large torsional amplitude motion has little effect on the structural parameters. In this way, the magnitudes of structural gradients can be taken as a qualitative measure of contributions of a part of a larger molecule to the vibrational entropy of the system.

In ALA-ALA a new aspect of TS can be investigated in that it is possible not only to study the TS within the moving residue, but also that of the constrained residue. That is, it is possible to illustrate the effects of small-amplitude torsional motions in one part of the molecule on the TS of another part. This is not only

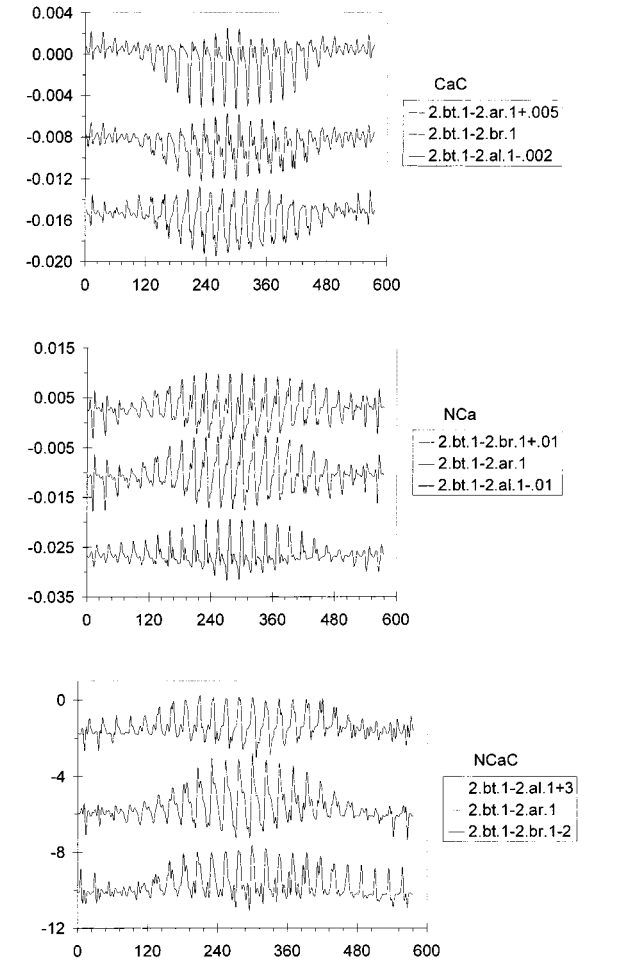

Figure 4. Differences between the surfaces 2.bt.1 and 2.ar.1, 2.br.1, and 2.al.1, respectively, for the bond distances C_α−C′ and N−C_α and the valence angle N−C_α−C′. The graphs show average values as functions of regions numbers in ϕ_1,ψ_1-space. Each region is a segment of a 15° grid in ϕ,ψ-space. Region numbering started with the segment $-180° \le \phi_1 \le -165°$, $-180° \le \psi_1 \le -165°$, and increased from −180° to 165°, moving along the ψ-axis first. In each region, values were calculated at 5° intervals, averaged, and the resulting values were plotted.

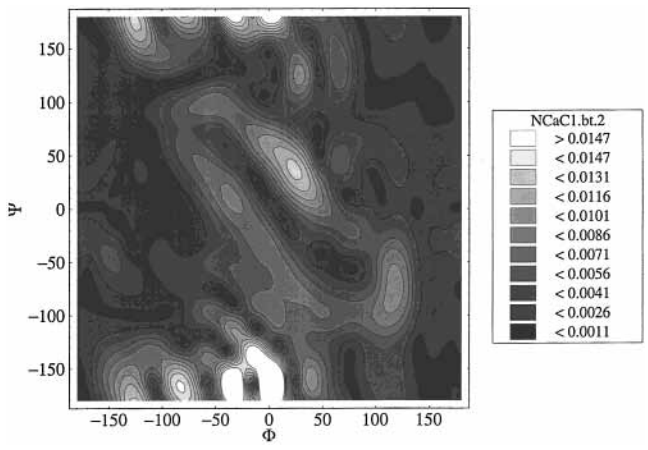

Figure 5. Gradient magnitude, $[(\partial N-C_\alpha-C'1.bt.2/\partial\phi_2)^2 + (\partial N-C_\alpha-C'1.bt.2/\partial\psi_2)^2]^{1/2}$, plotted as a function of ϕ_2 and ψ_2.

another test of the dipeptide approximation but also an illustration that the *dynamics* of one residue, not only its *static* properties, can have a significant effect on the density of states, or the contribution to system entropy, originating with another residue. It is conceivable that, in large systems, such interresidue

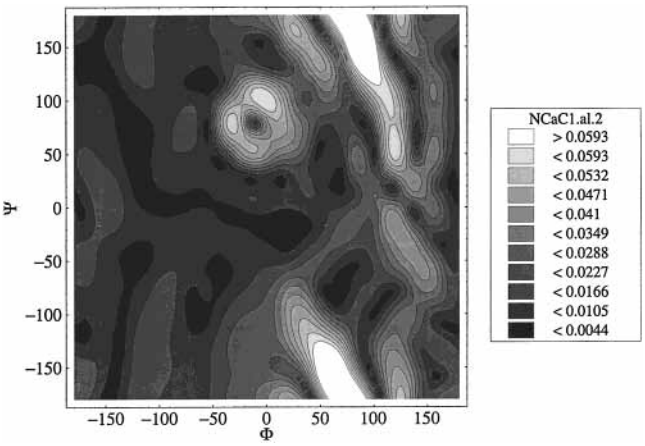

Figure 6. Gradient magnitude, $[(\partial N-C_\alpha-C'1.al.2/\partial\phi_2)^2 + (\partial N-C_\alpha-C'1.al.2/\partial\psi_2)^2]^{1/2}$, plotted as a function of ϕ_2 and ψ_2.

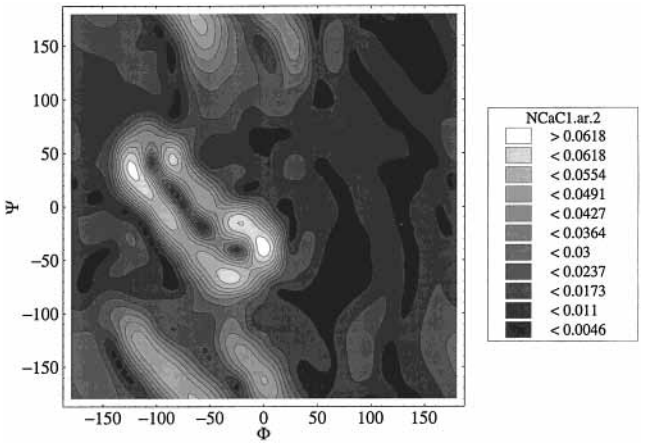

Figure 7. Gradient magnitude, $[(\partial N-C_\alpha-C'1.ar.2/\partial\phi_2)^2 + (\partial N-C_\alpha-C'1.ar.2/\partial\psi_2)^2]^{1/2}$, plotted as a function of ϕ_2 and ψ_2.

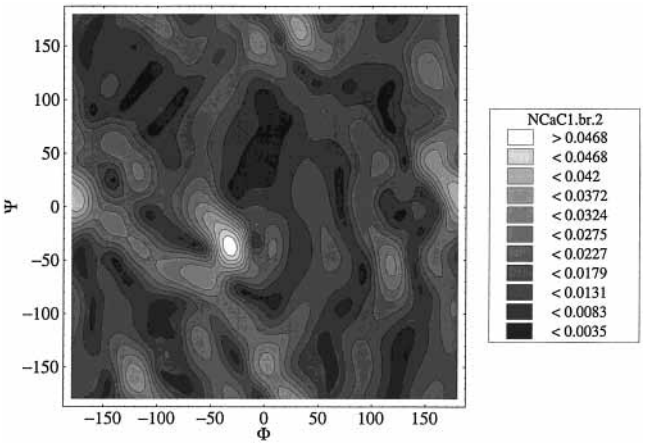

Figure 8. Gradient magnitude, $[(\partial N-C_\alpha-C'1.br.2/\partial\phi_2)^2 + (\partial N-C_\alpha-C'1.br.2/\partial\psi_2)^2]^{1/2}$, plotted as a function of ϕ_2 and ψ_2.

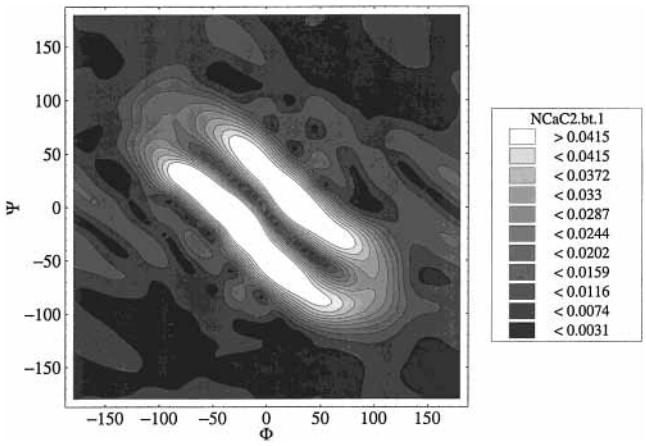

Figure 9. Gradient magnitude, $[(\partial N-C_\alpha-C'2.bt.1/\partial\phi_1)^2 + (\partial N-C_\alpha-C'2.bt.1/\partial\psi_1)^2]^{1/2}$, plotted as a function of ϕ_1 and ψ_1.

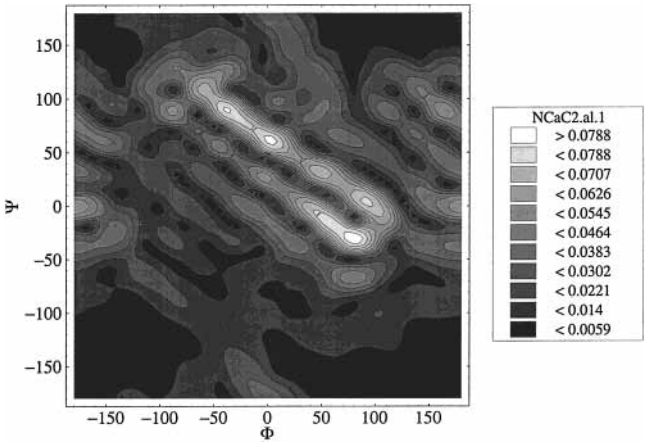

Figure 10. Gradient magnitude, $[(\partial N-C_\alpha-C'2.al.1/\partial\phi_1)^2 + (\partial N-C_\alpha-C'2.al.1/\partial\psi_1)^2]^{1/2}$, plotted as a function of ϕ_1 and ψ_1.

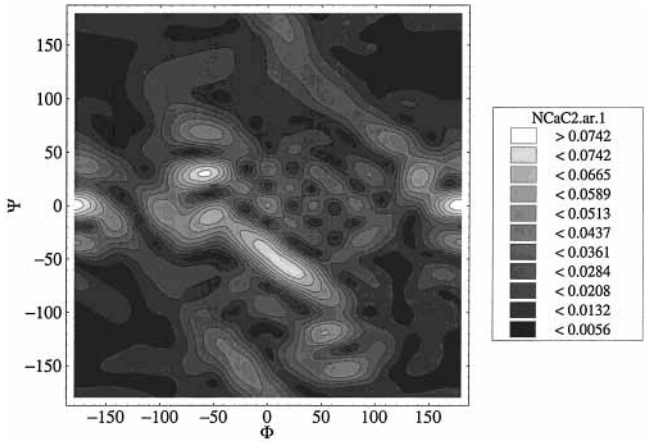

Figure 11. Gradient magnitude, $[(\partial N-C_\alpha-C'2.ar.1/\partial\phi_1)^2 + (\partial N-C_\alpha-C'2.ar.1/\partial\psi_1)^2]^{1/2}$, plotted as a function of ϕ_1 and ψ_1.

dynamic effects can contribute to entropic conformational steering, or the production of free energy contributions, which may help to stabilize the conformational region of a PES whose static energy is less favorable compared to other regions. These dynamic interresidue TS effects are entirely different in nature both from the constitutional intraresidue TS effects and from static interresidue energy effects.

In isolated model dipeptides, the structural gradients are usually high in the helical region of the PES and low in the β-region[55,56] due to intraresidue constitutional factors. The dynamic interresidue effects are entirely absent from all attempts to rationalize the conformational properties of oligopeptides and proteins on the basis of the dipeptide approximation.

Some typical gradient surfaces of ALA-ALA are shown in Figures 5−12. Comparing Figure 5 (gradient surface $N-C_\alpha-C'1.bt.2$) with Figure 6 ($N-C_\alpha-C'1.al.2$), Figure 7 ($N-C_\alpha-C'1.ar.2$), and Figure 8 ($N-C_\alpha-C'1.br.2$), it is seen that interresidue effects on the gradients of a residue differ significantly from one area of the PES of that residue to another. The same is found in the second series, Figures 9−12 ($N-C_\alpha-C'2.bt.1$, $N-C_\alpha-C'2.al.1$, $N-C_\alpha-C'2.ar.1$, $N-C_\alpha-C'2.br.1$, respectively). In each case, small-amplitude motions about ϕ

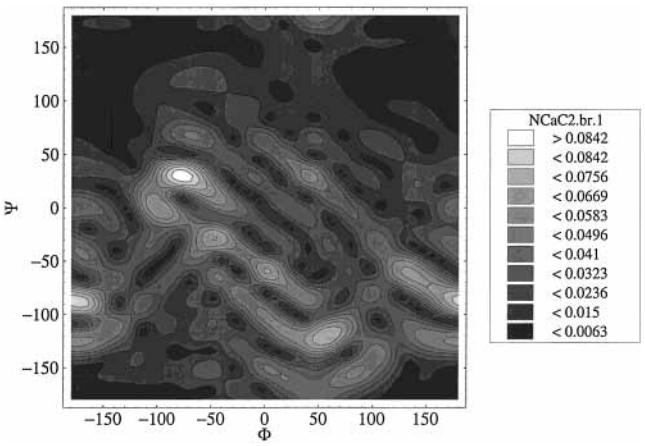

Figure 12. Gradient magnitude, $[(\partial N-C_\alpha-C'2.br.1/\partial\phi_1)^2 + (\partial N-C_\alpha-C'2.br.1/\partial\psi_1)^2]^{1/2}$, plotted as a function of ϕ_1 and ψ_1.

and ψ in one residue affect the structural gradients of the constrained residue in a way that depends on the conformational state of the latter.

Differences between corresponding curves in the two series of Figures, such as between Figure 5 ($N-C_\alpha-C'1.bt.2$) and Figure 9 ($N-C_\alpha-C'2.bt.1$), between Figure 6 ($N-C_\alpha-C'1.al.2$) and Figure 10 ($N-C_\alpha-C'2.al.1$), Figure 7 ($N-C_\alpha-C'1.ar.2$) and Figure 11 ($N-C_\alpha-C'2.ar.1$), and Figure 8 ($N-C_\alpha-C'1.br.2$) and Figure 12 ($N-C_\alpha-C'2.br.1$), indicate that the interresidue dynamic effects depend on whether they are transmitted from right to left or from left to right in the peptide chain. Similar results are obtained for other structural parameters, for example, the bond lengths and nonbonded distances, but they will not be reproduced here. In contrast, the structural gradients within the two residues of ALA-ALA are rather similar to each other and to the gradients of isolated ALA, when they are moving residues.

Conclusions

The results presented above show that an amino acid residue in a peptide chain can significantly influence its neighbor, illustrating the limitations of any procedure that attempts to use model dipeptides as ready-to-assemble building blocks for larger peptide chains.

Specifically, the bond lengths and bond angles of an amino acid residue in a peptide chain do not depend only on its own torsional ϕ,ψ-angles but also on the conformational state of neighboring residues. In ALA-ALA the magnitude of such effects can amount to several hundredths of an Å in bond lengths, and up to 4° for bond angles. Moreover, these interresidue effects differ, depending on whether they are transmitted from left to right or from right to left in the peptide chain.

In addition to static interresidue interactions, the density of states in a peptide bound amino acid residue, and thus its contribution to the vibrational entropy of the system, can be affected by the *dynamics* of neighboring residues. This opens the possibility of dynamic entropic conformational steering in extended peptide chains, i.e., the generation of free energy contributions from dynamic effects of one part of the molecule on another, which can help to stabilize the conformational region of a PES whose static energy profile is less favorable compared to other regions.

These results illustrate how the overall stability of a complex molecule is not only a function of how the static energy minima of its isolated subunits combine but also of how the dynamics of the subunits interact with each other. Traditionally, conformational analyses of oligopeptides and proteins have focused on the former and neglected the latter. Static energy effects in oligopeptides may to some extent be estimated from the static energy minima of isolated dipeptides, albeit not without problems, as pointed out above. But the interactions of the dynamics and their effects between individual residues represent a hidden cooperative effect that is not apparent at all in the dynamics of isolated dipeptide units.

Apart from the considerations presented above, the quantitative structural information given in the ALA-ALA database can be used in parameter refinements for empirical molecular modeling procedures. In our group, for example, they are currently being applied in attempts to improve molecular dynamics simulation procedures of the adsorption of organic materials on the clay mineral/aqueous solution interface.[69,70]

Acknowledgment. The authors gratefully acknowledge partial support of this work by U.S. Department of Agriculture National Research Incentive Grant 97-35107-4362.

References and Notes

(1) Ryan, J. A.; Whitten, J. L. *J. Am. Chem. Soc.* **1972**, *94*, 2396.
(2) Peters, D.; Peters, J. *J. Mol. Struct.* **1980**, *68*, 243.
(3) Ramani, R.; Boyd, R. J. *Int. J. Quantum Chem. Quantum Biol. Symp.* **1981**, *8*, 117.
(4) Wright, L. R.; Borkman, R. F. *J. Phys. Chem.* **1982**, *86*, 3956.
(5) Sapse, A.-M.; Daniels, S. B.; Erickson, B. W. *Tetrahedron* **1988**, *44*, 999.
(6) Mavri, J.; Avbelj, F.; Hadñi, D. *J. Mol. Struct. (Theochem)* **1989**, *187*, 307.
(7) Sapse, A.-M.; Jain, D. C.; de Gale, D.; Wu, T. C. *J. Comput. Chem.* **1990**, *11*, 573.
(8) Böhm, H.-J. *J. Am. Chem. Soc.* **1993**, *115*, 6152.
(9) Antohi, O.; Naider, F.; Sapse, A.-M. *J. Mol. Struct. (Theochem)* **1996**, *360*, 99.
(10) Antohi, O.; Sapse, A.-M. *J. Mol. Struct. (Theochem)* **1998**, *430*, 247.
(11) Perczel, A.; Kajtár, M.; Marcoccia, J.-F.; Csizmadia, I. G. *J. Mol. Struct. (Theochem)* **1991**, *232*, 291.
(12) Möhle, K.; Gussmann, M.; Hofmann, H.-J. *J. Comput. Chem.* **1997**, *18*, 1415.
(13) McAllister, M. A.; Perczel, A.; Császár, P.; Csizmadia, I. G. *J. Mol. Struct. (Theochem)* **1993**, *288*, 181.
(14) Peters, D.; Peters, J. *J. Mol. Struct. (Theochem)* **1981**, *85*, 267.
(15) Gresh, N.; Tiraboschi, G.; Salahub, D. R. *Biopolymers* **1998**, *45*, 405.
(16) Perczel, A.; Endredi, G.; McAllister, M. A.; Farkas, O.; Császár, P.; Ladik, J.; Csizmadia, I. G. *J. Mol. Struct. (Theochem)* **1995**, *331*, 5.
(17) Schäfer, L.; Newton, S. Q.; Cao, M.; Peeters, A.; Van Alsenoy, C.; Wolinski, K.; Momany, F. A. *J. Am. Chem. Soc.* **1993**, *115*, 272.
(18) Perczel, A.; McAllister, M. A.; Császár, P.; Csizmadia, I. G. *J. Am. Chem. Soc.* **1993**, *115*, 4849.
(19) Van Alsenoy, C.; Cao, M.; Newton, S. Q.; Teppen, B.; Perczel, A.; Csizmadia, I. G.; Momany, F. A.; Schäfer, L. *J. Mol. Struct.* **1993**, *286*, 149.
(20) Perczel, A.; McAllister, M. A.; Császár, P.; Csizmadia, I. G. *Can. J. Chem.* **1994**, *72*, 2050.
(21) Ramek, M.; Yu, C.-H.; Schäfer, L. *Can. J. Chem.* **1998**, *76*, 566.
(22) Shipman, L. L.; Christoffersen, R. E. *J. Am. Chem. Soc.* **1973**, *95*, 4733.
(23) Kleier, D. A.; Lipscomb W. N. *Int. J. Quantum Chem. Quantum Biol. Symp.* **1977**, *4*, 73.
(24) Peters, D.; Peters, J. *J. Mol. Struct.* **1980**, *68*, 255.
(25) Peters, D.; Peters, J. *J. Mol. Struct.* **1980**, *69*, 249.
(26) Kertész, M., Koller, J.; Azman A. *Int. J. Quantum Chem. Quantum Biol. Symp.* **1980**, *7*, 177.
(27) Day, R. S.; Suhai, S.; Ladik, *Chem. Phys.* **1981**, *62*, 165.
(28) van Duijnen, P. T.; Thole B. T. *Biopolymers* **1982**, *21*, 1749.
(29) Suhai, S. *J. Mol. Struct. (Theochem)* **1985**, *123*, 97.
(30) Skála, L.; Pancoska P. *Chem. Phys.* **1988**, *125*, 21.
(31) Bakhshi, A. K.; Otto, P.; Ladik, J. *J. Mol. Struct. (Theochem)* **1988**, *180*, 113.
(32) Liegener, C.-M.; Bakhshi, A. K.; Otto, P.; Ladik, J. *J. Mol. Struct. (Theochem)* **1989**, *188*, 205.

(33) Bakhshi, A. K.; Otto, P.; Liegener, C.-M.; Rehm, E.; Ladik, J. *Int. J. Quantum Chem.* **1990**, *38*, 573.
(34) Barone, V.; Fraternali, F.; Cristinziano, P. L. *Macromolecules* **1990**, *23*, 2038.
(35) Liegener, C.-M.; Sutjianto, A.; Ladik, *Chem. Phys.* **1990**, *145*, 385.
(36) Otto, P.; Sutjianto, A. *J. Mol. Struct. (Theochem)* **1991**, *231*, 277.
(37) Chang, C.; Bader, R. F. W. *J. Phys. Chem.* **1992**, *96*, 1654.
(38) Torii, H.; Tasumi, M. *J. Mol. Struct.* **1993**, *300*, 171.
(39) Zhang, K.; Zimmerman, D. M.; Chung-Phillips, A.; Cassady, C. J. *J. Am. Chem. Soc.* **1993**, *115*, 10812.
(40) Walker, P. D.; Mezey, P. G. *J. Am. Chem. Soc*. **1993**, *115*, 12423.
(41) Walker, P. D.; Mezey, P. G. *J. Am. Chem. Soc*. **1994**, *116*, 12022.
(42) Endredi, G.; Liegener, C.-M.; McAllister, M. A.; Perczel, A.; Ladik, J.; Csizmadia, I. G. *J. Mol. Struct. (Theochem)* **1994**, *306*, 1.
(43) Sasisekharan, V. In *Collagen*; Ramanathan, N., Ed.; Interscience Publishers: New York, 1962; p 39.
(44) Ramachandran, G. N.; Ramakrishnan, C.; Sasisekharan, V. *J. Mol. Biol.* **1963**, *7*, 95.
(45) Ramakrishnan, C.; Ramachandran, G. N. *Biophys. J.* **1965**, *5*, 909.
(46) Leach, S. J.; Nemethy, G.; Scheraga, H. A. *Biopolymers* **1966**, *4*, 369.
(47) Gibson, K. D.; Scheraga, H. A. *Biopolymers* **1966**, *4*, 709.
(48) Ponnuswamy, P. K.; Sasisekharan, V. *Biopolymers* **1971**, *10*, 565.
(49) Ramachandran, G. N.; Venkatachalam, C. M.; Krimm, S. *Biophys. J.* **1966**, *6*, 849.
(50) Lewis, P. N.; Momany, F. A.; Scheraga, H. A. *Isr. J. Chem.* **1973**, *11*, 121.
(51) Pullman, B.; Pullman, A. *Adv. Protein Chem.* **1974**, *28*, 347.
(52) Binkley, J. S.; Pople, J. A.; Hehre, W. J. *J. Am. Chem. Soc*. **1980**, *102*, 939.
(53) Pulay, P.; Fogarasi, G.; Pang, F.; Boggs, J. E. *J. Am. Chem. Soc*. **1979**, *101*, 2550.
(54) Schäfer, L.; Van Alsenoy, C.; Scarsdale, J. N. *J. Chem. Phys.* **1982**, *76*, 1439.
(55) Cao, M.; Schäfer, L. *J. Mol. Struct.* **1993**, *284*, 235.
(56) Yu, C.-H.; Schäfer, L.; Ramek, M,; Miller, D. M.; Teppen, B. J. *J. Mol. Struct.* **1999**, *485*−*486*, 373.
(57) Hehre, W. J.; Ditchfield, R.; Pople, J. A. *J. Chem. Phys*. **1972**, *56*, 2257.
(58) Hariharan, P. C.; Pople, J. A. *Theor. Chim. Acta* **1973**, *28*, 213.
(59) Marsh, R. E.; Donohue, J. *Adv. Protein Chem*. **1967**, *22*, 235.
(60) Corey, R. B.; Pauling, L. *Proc. R. Soc. London Ser. B* **1953**, *141*, 10.
(61) Scheraga, H. A. *Adv. Phys. Org. Chem*. **1968**, *6*, 103.
(62) Pople, J. A.; Gordon, M. *J. Am. Chem. Soc*. **1967**, *89*, 4253.
(63) Karplus, P. A. *Protein Sci.* **1996**, *5*, 1406.
(64) Frey, R. F.; Coffin, J.; Newton, S. Q.; Ramek, M.; Cheng, V. K. W.; Momany, F. A.; Schäfer, L. *J. Am. Chem. Soc.* **1992**, *114*, 5369.
(65) Schäfer, L.; Van Alsenoy, C.; Scarsdale, J. N. *J. Mol. Struct.* **1982**, *86*, 349.
(66) de Smedt, J.; Vanhouteghem, F.; Van Alsenoy, C.; Geise, H. J.; Schäfer, L. *J. Mol. Struct.* **1992**, *259*, 289.
(67) Schäfer, L.; Cao, M.; Meadows, M. *J. Biopol*. **1994**, *35*, 603.
(68) Jiang, X.; Cao, M.; Teppen, B.; Newton, S. Q.; Schäfer, L. *J. Phys. Chem.* **1995**, *99*, 10521.
(69) Teppen, B. J.; Rasmussen, K.; Bertsch, P. M.; Miller, D. M.; Schäfer, L. *J. Phys. Chem.* **1997**, *101*, 1579.
(70) Teppen, B. J.; Yu, C.-H.; Miller, D. M.; Schäfer, L. *J. Comput. Chem*. **1998**, *19*, 144.